Finite-size analysis of the hard-square lattice gas

Wenan Guo[1] and Henk W. J. Blöte[2]
[1]*Physics Department, Beijing Normal University, Beijing 100875, People's Republic of China*
[2]*Faculty of Applied Sciences, Delft University of Technology, P.O. Box 5046, 2600 GA Delft, The Netherlands and Lorentz Institute, Leiden University, P.O. Box 9506, 2300 RA Leiden, The Netherlands*
(Received 19 January 2002; revised manuscript received 26 August 2002; published 30 October 2002)

We investigate the hard-square lattice-gas model by means of transfer-matrix calculations and a finite-size-scaling analysis. Using a minimal set of assumptions we find that the spectrum of correction-to-scaling exponents is consistent with that of the exactly solved Ising model, and that the critical exponents and correlation-length amplitudes closely follow the relation predicted by conformal invariance. Assuming that these spectra are exactly identical, and conformal invariance, we determine the critical point, the conformal anomaly, and the temperature and magnetic exponents with numerical margins of 10^{-11} or less. These results are in a perfect agreement with the exactly known Ising universal parameters in two dimensions. In order to obtain this degree of precision, we included system sizes as large as feasible, and used extended-precision floating-point arithmetic. The latter resource provided a substantial improvement of the analysis, despite the fact that it restricted the transfer-matrix calculations to finite sizes of at most 34 lattice units.

DOI: 10.1103/PhysRevE.66.046140 PACS number(s): 64.60.Cn, 64.60.Fr, 05.50.+q, 75.10.Hk

I. INTRODUCTION

Hard-core lattice gases can be seen as limiting cases of antiferromagnetic Ising models in a field. Here we consider the model on the square lattice

$$\mathcal{H}/kT = -K\sum_{x,y} s_{x,y}(s_{x+1,y}+s_{x,y+1}) - H\sum_{x,y} s_{x,y}, \quad (1)$$

with spin coordinates x,y subject to periodic boundary conditions. The antiferromagnetic transition at $K=-\frac{1}{2}\ln(1+\sqrt{2})$ is stable under the application of a magnetic field, and belongs to a critical line spanning the range $-\infty<H<\infty$. The model has not been solved in a nonzero field, but the critical line is accurately known [1].

The lattice-gas model applies in the limit where both H and $-K$ become infinite, but balancing one another such that the fully magnetized phase competes with the antiferromagnetic phase. In this limit, a spin can be oriented in opposition to the field only if its four nearest neighbors are parallel to the field. Obviously $H+4K$ must remain finite in this situation. The allowed Ising configurations can equivalently be interpreted in terms of lattice-gas variables $\sigma_{x,y}=(1-s_{x,y})/2$ where $\sigma_{x,y}=1$ represents the presence of a particle, and $\sigma_{x,y}=0$ its absence. This transformation leads to

$$\mathcal{H}/kT = -\sum_{x,y} \sigma_{x,y}\ [\mu+4K(\sigma_{x+1,y}+\sigma_{x,y+1})], \quad (2)$$

where we have omitted an additional constant, and $\mu=-(8K+2H)$ is the chemical potential of the lattice-gas particles. For $K\to-\infty$ we have nearest-neighbor exclusion: a pair of occupied neighbor sites contributes an infinite amount of energy. This condition can be graphically depicted by assigning diagonally oriented squares to each particle, with a diagonal size of two lattice units. These hard squares cannot overlap. Apart from this infinite hard-core potential, they do not interact. It is noteworthy that, in this sense, the model differs from Fisher's [2] and Baxter's [3,4] hard-square models. To emphasize the difference, the somewhat imprecise adjective ''noninteracting'' has sometimes been used for the model (2) with $K\to-\infty$. In this work, we simply refer to it as ''the hard-square lattice gas.''

For a sufficiently large chemical potential μ, the model undergoes an ordering transition where the majority of the lattice-gas particles settle on one of the two checkerboard sublattices. The order parameter is defined as the occupation difference between the two sublattices. Since it is a scalar, just as in the ordinary Ising model, one may, on the basis of the principle of universality, conjecture that the universal parameters of the hard-square lattice-gas model are *exactly* those of the Ising model. This conjecture is also in line with Fisher's [2] exact solution of a related lattice-gas model.

In the absence of an exact solution of the model (2), there exists a long and interesting history of numerical efforts to test this conjecture. An early series-expansion analysis by Gaunt and Fisher [5] yielded $\beta=0.125\pm0.005$ for the magnetization exponent, in a good agreement with the exact Ising value $\beta=1/8$. This result already greatly restricted any possible deviations from Ising universality. Further restrictions could follow from an accurate determination of a second critical exponent. However, series expansions by Baxter *et al.* [6] surprisingly yielded $\alpha=0.09\pm0.05$ for the specific-heat exponent, while $\alpha=0$ for the exactly solved Ising model. The numerical result for α could thus be interpreted as mild evidence *against* Ising universality. Although Baxter *et al.* explicitly added the statement that Ising exponents were not excluded, their result has received considerable attention, and led to a series of numerical investigations [7–10] aiming at much more precise tests of the hypothesis that the hard-square lattice gas belongs to the Ising universality class. The results were strongly in favor of this hypothesis; results for the scaling dimensions, reported by Kamieniarz and Blöte [9] and by Todo and Suzuki [10] agree with the Ising values within numerical margins of 10^{-6} and 10^{-7}, respectively.

Nevertheless one can still ask the question whether solvable Ising models have some physical characteristics in common that are not shared by a class of other Ising-like models, which includes the present hard-square model, so that we may use that model as a test case. While there is no compelling reason to doubt the general validity of the renormalization theory, which forms the basis of the universality hypothesis, a rigorous justification is absent. Moreover, specific applications are subject to significant difficulties; see, e.g., Refs. [11–13].

For this reason we have revisited the hard-square lattice gas, aiming at a considerably more sensitive test of universality. In Sec. II we describe the transfer-matrix technique used to generate the numerical data for the finite-size-scaling analysis described in Sec. III. Section III A confirms that the critical finite-size amplitude of the magnetic correlation length, and the correction-to-scaling exponents are consistent with those of the Ising universality class. Then, under the assumption that these parameters fit the Ising class *exactly*, we perform another determination of the critical point and other parameters. This procedure enables the detection of extremely small deviations from universality. However, the results, which are briefly discussed in Sec. IV, agree precisely with the known universal Ising parameters. The analyses include a test of conformal invariance, by means of two independent determinations of the critical exponents using transfer-matrix methods. The first method (Sec. III E) uses numerical differentiations of the free energy and the correlation length to the chemical potential and to the staggered field. The second method uses the relation between critical exponents and correlation lengths in a cylinder geometry, as based on the assumption of conformal invariance. These two methods lead to identical results and are thus in support of the assumption made.

II. THE TRANSFER MATRIX

We analyze the lattice-gas model on a square $L\times m$ lattice with periodic boundary conditions in the direction with system size L. Thus the sites of the lattice are divided in m circular rows. There are free boundaries in the other direction. According to Eq. (2) with $K\to-\infty$, the partition sum is

$$Z^{(m)}=\sum_{\{\sigma_i\}} e^{\mu\sum_i \sigma_i}\prod_{\langle i,j\rangle}(1-\sigma_i\sigma_j), \tag{3}$$

where μ is the reduced chemical potential, and m has been added explicitly to indicate the number of rows. Next, we divide $Z^{(m)}$ in a number of restricted sums, each of which corresponds with a given state of the particles in the mth row. We denote the particle configuration of row i as $\vec{\sigma}_i=(\sigma_{i,1},\sigma_{i,2},\ldots,\sigma_{i,L})$, so that the restricted sums are

$$Z^{(m)}(\vec{\sigma}_m)=\sum_{\vec{\sigma}_1}\sum_{\vec{\sigma}_2}\cdots\sum_{\vec{\sigma}_{m-1}}\left[\prod_{n=1}^{m}\prod_{k=1}^{L} e^{\mu\sigma_{n,k}}(1-\sigma_{n,k}\sigma_{n-1,k})\times(1-\sigma_{n,k}\sigma_{n,k+1})\right], \tag{4}$$

with $\sigma_{n,L+1}\equiv\sigma_{n,1}$ and $\sigma_{0,k}\equiv 0$. The restricted sums for a system of $m+1$ rows are

$$Z^{(m+1)}(\vec{\sigma}_{m+1})=\sum_{\vec{\sigma}_m}\left\{\sum_{\vec{\sigma}_1}\sum_{\vec{\sigma}_2}\cdots\sum_{\vec{\sigma}_{m-1}}\left[\prod_{n=1}^{m}\prod_{k=1}^{L} e^{\mu\sigma_{n,k}}\times(1-\sigma_{n,k}\sigma_{n-1,k})(1-\sigma_{n,k}\sigma_{n,k+1})\right]\right\}\times\prod_{k=1}^{L} e^{\mu\sigma_{m+1,k}}(1-\sigma_{m+1,k}\sigma_{m,k})\times(1-\sigma_{m+1,k}\sigma_{m+1,k+1}). \tag{5}$$

Using the definition of $Z^{(m)}(\vec{\sigma}_m)$, and that of the transfer matrix as

$$\tilde{T}(\vec{\sigma}_{m+1},\vec{\sigma}_m)\equiv\prod_{k=1}^{L} e^{\mu\sigma_{m+1,k}}(1-\sigma_{m,k}\sigma_{m,k+1})\times(1-\sigma_{m+1,k}\sigma_{m,k})(1-\sigma_{m+1,k}\sigma_{m+1,k+1}), \tag{6}$$

one obtains

$$Z^{(m+1)}(\vec{\sigma}_{m+1})=\sum_{\vec{\sigma}_m}\tilde{T}(\vec{\sigma}_{m+1},\vec{\sigma}_m)Z^{(m)}(\vec{\sigma}_m). \tag{7}$$

In vector notation, iteration of this recursion yields

$$\vec{Z}^{(m+1)}=\tilde{\mathbf{T}}\cdot\vec{Z}^{(m)}=[\tilde{\mathbf{T}}]^m\cdot\vec{Z}^{(1)}. \tag{8}$$

Expansion of $\vec{Z}^{(1)}$ in right-hand eigenvectors of $\tilde{\mathbf{T}}$ shows that

$$Z^{(M)}=\sum_{\vec{\sigma}} Z^{(M)}(\vec{\sigma})=\sum_i c_i\lambda_i^M, \tag{9}$$

where the c_i are constants and the λ_i the eigenvalues of $\tilde{\mathbf{T}}$. Thus the reduced free energy $f(L)$ per site in the large-M limit is

$$f(L)=\lim_{M\to\infty}\frac{1}{LM}\ln Z^{(M)}=\frac{1}{L}\ln\lambda_0, \tag{10}$$

where λ_0 is the largest eigenvalue of $\tilde{\mathbf{T}}$.

To facilitate the numerical analysis, we define the elements of a symmetric version $\mathbf{T}$ of the transfer matrix by a similarity transformation

$$T(\vec{\sigma}_{m+1},\vec{\sigma}_m)\equiv\prod_{k=1}^{L} e^{\mu(\sigma_{m,k}-\sigma_{m+1,k})/2}\ \tilde{T}(\vec{\sigma}_{m+1},\vec{\sigma}_m). \tag{11}$$

To enable actual transfer-matrix calculations, we have to assign unique numbers to the particle configurations of a single row. This coding thus serves to define the transfer-matrix indices. It is natural to use a coding by means of the binary number $\sigma_1\sigma_2\cdots\sigma_L$, but this is not an efficient cod-

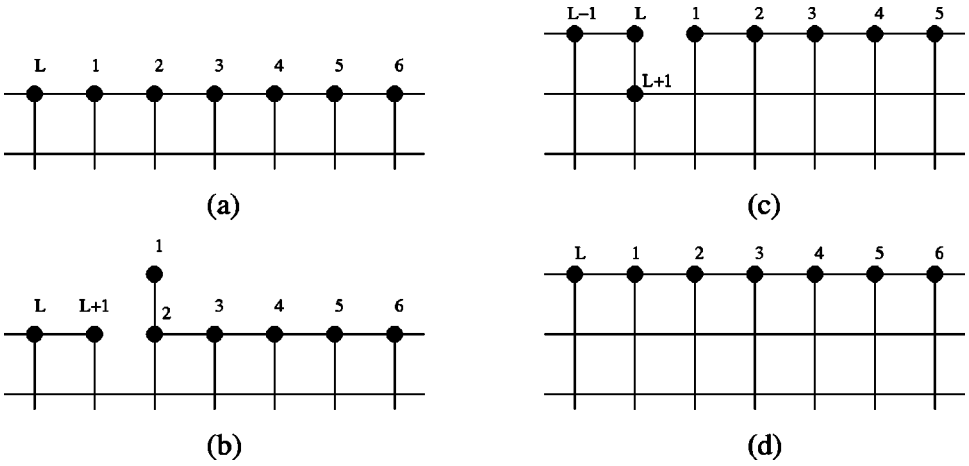

FIG. 1. Illustration of the action of the sparse matrices composing the transfer matrix. A part of the topmost rows of the square lattice is shown (a) after completion of a new row, (b) after appending a new site by $\mathbf{T}_1$, (c) after appending the Lth new site by $\mathbf{T}_L$, and (d) after deleting the site labeled $L+1$ and shifting the site numbers by $\mathbf{T}_{L+1}$.

ing, because it includes configurations with occupied neighbor sites. These configurations have a zero weight, due to the presence of the infinite hard-core potential. Following Todo and Suzuki [10] we use an enumeration that includes allowed configurations only. Let n_{σ_1,L,σ_L} denote the number of allowed configurations on a row of L sites with given σ_1 and σ_L. These numbers satisfy the recursions

$$n_{0,L+1,0}=n_{0,L,0}+n_{0,L,1}, \quad n_{0,L+1,1}=n_{0,L,0} \tag{12}$$

so that $n_{0,L+1,0}=n_{0,L,0}+n_{0,L-1,0}$. Since we have $n_{0,1,0}=1$ and $n_{0,2,0}=1$, the number $n_{0,L,0}$ is just the Lth Fibonacci number $F_{1,1}(L)$ of the sequence starting with 1, 1. Furthermore we find $n_{0,L,1}=F_{0,1}(L)$. On the basis of symmetry we also have $n_{1,L,0}=n_{0,L,1}$ so that the total number $n_c(L)$ of allowed configurations on a circular row of L sites

$$n_c(L)=n_{0,L,0}+n_{1,L,0}+n_{0,L,1}=F_{1,1}(L)+2F_{0,1}(L)=F_{1,3}(L) \tag{13}$$

is the Lth number of the Fibonacci sequence starting with 1 and 3. For large L this number is much smaller than 2^L which applies to the binary coding. In order to assign a unique number to each specific configuration, we need only define an ordering of the $F_{1,3}(L)$ possible configurations. This ordering can be conveniently taken identical to the ordering of the corresponding binary numbers. This defines the coding of the $F_{1,3}(L)$ allowed configurations.

To reduce the memory and the computer time requirements, the transfer matrix is decomposed in $L+1$ sparse matrices

$$\mathbf{T}=\mathbf{T}_{L+1}\cdot\mathbf{T}_L\cdots\mathbf{T}_2\cdot\mathbf{T}_1, \tag{14}$$

where $\mathbf{T}_1$ acts as to add a new site to a complete row. More precisely, it renames site 1 as $L+1$, and it places a new site with number 1 above site number 2. Since sites 1 and $L+1$ are not nearest neighbors, one obtains a row of $L+1$ sites with open boundaries [see Figs. 1(a) and (b)]. A slightly different coding algorithm has therefore to be used. Each of the matrices $\mathbf{T}_2,\ldots,\mathbf{T}_L$ adds an elementary square to the lattice, i.e., it replaces an old site by a new site which is added diagonally, as shown in Fig. 1(c) for $\mathbf{T}_L$. Finally $\mathbf{T}_{L+1}$ disposes of site $L+1$, constructs a bond (i.e., imposes the nearest-neighbor exclusion constraint) between sites L and 1, and then translates the site label by one unit as shown in Fig. 1(d). Further details of numerical transfer-matrix techniques in general were given by e.g., Nightingale [14], and for the present case of the hard-core lattice gas by Todo and Suzuki [10].

The transfer matrix is symmetric, which enables the use of the conjugate-gradient algorithm to compute some of its eigenvalues $\lambda_i (i=1,2,\ldots)$, and their associated eigenvectors $\vec{e}_i$. The iterative procedure to find the largest eigenvalue λ_0 starts from an initial vector that is translationally invariant (i.e., under cyclic permutations of the site number) as well as invariant under a geometric inversion, i.e., an interchange of the site labels $k\leftrightarrow L+1-k$. The corresponding eigenvector $\vec{e}_0$ satisfies these symmetries, as a consequence of the symmetry properties of $\mathcal{H}$ and the Perron-Frobenius theorem. The second largest (in absolute value) eigenvalue is denoted λ_1. Just as in the Ising model, its ratio with respect to the largest eigenvalue determines a correlation length of the ''magnetic'' type, i.e., it pertains to the staggered particle, density. The associated eigenvector $\vec{e}_1$ is antisymmetric under a geometric inversion. Therefore the iterations started from an antisymmetric initial vector, and precautions were taken to prevent the buildup of a symmetric component due to the finite numerical precision of the iterative multiplication process. Furthermore we computed a third eigenvalue λ_2, namely, the second largest eigenvalue in the symmetric subspace. Its gap with respect to λ_0 determines the correlation length associated with the energy-energy correlation function. This eigenvalue was obtained using a symmetric initial vector, and orthogonalization with respect to $\vec{e}_0$.

In general one can relate a subleading eigenvalue λ_i of $\mathbf{T}$ to the correlation length associated with an appropriate correlation function. In the case of even L, the inverse correlation lengths $\xi_i^{-1}(L)$ are equal to

$$\xi_i^{-1}(L)=\ln\frac{\lambda_0}{|\lambda_i|}, \tag{15}$$

where the case $i=1$ applies to the magnetic correlation length ξ_h while $i=2$ applies to the energy-energy correlation

length ξ_t. We restrict L to be even because the ground state does not fit a lattice with odd L, in which case the scaling behavior is modified.

The expectation value of the particle density ρ is determined by the eigenvector $\vec{e}_0$ associated with λ_0. To this purpose we define a diagonal matrix $\mathbf{D}$ with elements $D_{\vec{\sigma}_i,\vec{\sigma}_j} = \delta_{\vec{\sigma}_i,\vec{\sigma}_j} \Sigma_{k=1}^{L} \sigma_{i,k}$ so that $\rho = \vec{e}_0 \cdot \mathbf{D} \cdot \vec{e}_0$.

Next we describe how the definition of the transfer matrix is adapted to include a ''staggered field'' or a staggered contribution $\mu_{\rm st}$ to the chemical potential. The chemical potential is then $\mu+\mu_{\rm st}$ for particles on one sublattice, and $\mu-\mu_{\rm st}$ on the other. The staggered chemical potential can straightforwardly be included in Eqs. (6) and (11). However, since the contributions of $\mu_{\rm st}$ per site alternate between subsequent rows, the definition of $\mathbf{T}$ must be adapted to append *two* rows at a time. Another technical problem, namely, that the above-mentioned geometric inversion symmetry is destroyed by a nonzero staggered field, so that the second eigenvector can no longer be selected on the basis of this symmetry, can be solved by orthogonalization with respect to the eigenvector associated with the largest eigenvalue λ_0.

III. NUMERICAL RESULTS

We performed calculations up to $L=36$; the transfer matrix is then 33,385,282 dimensional. These calculations used standard double-precision arithmetic. However, as a consequence of this limitation of the numerical accuracy, these failed to provide a significant improvement over existing results. First, the iterative process to obtain the eigenvalues, which involves linear operations on long vectors, already induces a loss of accuracy of a few decimal places, and second, the inaccuracy is further enlarged during each step of the subsequent iterated fitting procedures. For this reason we have performed the transfer-matrix calculations as well as the subsequent fits in quadruple precision (16-byte) floating-point arithmetic as available on the Cray J-90 computer of the HPaC center in Delft. Its 2480 Mbyte of available memory restricted the finite-size calculations to $L \leqslant 34$. Although this range of finite sizes does not exceed that used in a recent analysis [10], the higher precision of the eigenvalues allows one to account for additional corrections to the leading scaling behavior, and thus leads to more precise results.

A. Preliminary analysis

We first use minimal assumptions, without *a priori* knowledge of critical exponents and amplitudes, to estimate the critical value of the chemical potential and a few other parameters that play a role in the finite-size behavior of the correlation length. This is done by means of an analysis of the L and μ dependence of the magnetic scaled gap $X_h(\mu,L)$, defined as $X_h(\mu,L)=L/[2\pi\xi_h(L)]$. For small $t=\mu-\mu_c$, i.e., close to the critical point, finite-size scaling [15] suggests the following behavior:

$$X_h(\mu,L) = X_h + atL^{y_t} + bL^{y_i} + \cdots, \tag{16}$$

where X_h is an (in principle) unknown number related to the finite-size amplitude of the correlation length, and the temperature exponent y_t and the irrelevant exponent y_i are likewise unknown. In addition one may expect corrections with higher powers of t and $1/L$. Let us now consider the difference

$$X_h(\mu,L+1) - X_h(\mu,L-1) = 2L^{-1}(aty_tL^{y_t} + by_iL^{y_i} + \cdots). \tag{17}$$

Since we have an algorithm to compute $X_h(\mu,L)$, we can apply ''phenomenological renormalization'' [14], i.e., numerically solve for μ in $X_h(\mu,L+1)-X_h(\mu,L-1)=0$. The solutions, which are denoted $\mu^{(0)}(L)$, agree with earlier numerical results [1,10]. These data, truncated to seven decimal places, are shown in Table I. For system sizes up to $L=33$, they already suggest convergence up to the fifth decimal place. The same data, but in quadruple precision, are presented in Table I in Ref. [16]. According to finite-size scaling they behave as

$$\mu^{(0)}(L) = \mu_c + by_iL^{y_i-y_t/(ay_t)} + \cdots. \tag{18}$$

This suggests that even better estimates of the critical point are obtained by a three-point fit with a variable exponent: solving for the unknowns $\mu^{(1)}(L)$, b_1, and x_1 in

$$\mu^{(0)}(L+l) = \mu^{(1)}(L) + b_1(L+l)^{x_1}, \tag{19}$$

for $l=0$ and ± 2. Indeed we then find an even faster apparent convergence to the critical point. Moreover, the results for the exponent x_1 provide a strong sign that $x_1=y_i-y_t=-3$, just as in the exactly solved Ising model. The solutions for x_1 are found to approach the value -3 within 5×10^{-2} in the available range of finite sizes.

TABLE I. Numerical solutions $\mu^{(0)}(L)$ of the equation $X_h(\mu,L-1)=X_h(\mu,L+1)$ for different system sizes L, and the corresponding values of X_h.

L	$\mu^{(0)}(L)$	$X_h^{(0)}(L)$
3	1.411 266 7	0.110 726 3
5	1.349 010 5	0.120 460 6
7	1.339 357 0	0.122 760 5
9	1.336 487 4	0.123 673 6
11	1.335 350 4	0.124 126 2
13	1.334 814 7	0.124 382 1
15	1.334 530 6	0.124 540 5
17	1.334 366 4	0.124 645 1
19	1.334 265 0	0.124 717 7
21	1.334 199 1	0.124 770 2
23	1.334 154 5	0.124 809 3
25	1.334 123 2	0.124 839 2
27	1.334 100 6	0.124 862 6
29	1.334 083 8	0.124 881 3
31	1.334 071 2	0.124 896 4
33	1.334 061 5	0.124 908 8

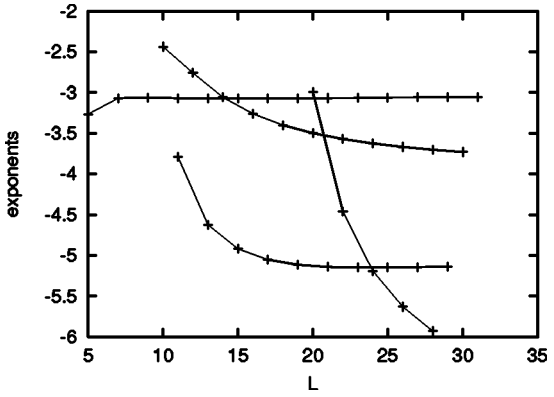

FIG. 2. Exponents x_i (Eq. 20) of finite-size corrections in the solutions $\mu^{(0)}$ of the equation $X_h(\mu^{(0)},L-1)=X_h(\mu^{(0)},L+1)$, versus finite size L. The correction exponents were estimated in several iteration steps in the analysis. Starting from above, the first line shows the exponent of the leading finite-size correction revealed by a three-point fit to the values of $\mu^{(0)}$. It indicates that the dominant correction is proportional to L^{-3}. The second line displays the result of the second iteration step, which was based on a fit using a fixed exponent -3 as a first step. It suggests that the next exponent is -4. Assuming this value, the next iteration yields the third line which shows that the next exponent is close to -5. Then, assuming exponents -3, -4, and -5, we obtain the fourth line that is consistent with a correction exponent -6.

We therefore assume that $x_1=-3$ holds exactly, and attempt to resolve the next correction exponent x_2 in the expansion

$$\mu^{(0)}(L)=\mu_c+b_1L^{x_1}+b_2L^{x_2}+b_3L^{x_3}+\cdots. \tag{20}$$

A fit involving the correction term $b_2L^{x_2}$ suggests that $x_2=-4$, although this exponent cannot be determined as precisely as x_1, apparently because the amplitude b_2 is relatively small.

Thus we assume $x_2=-4$ and try to find the next exponent x_3. This is done by means of a first fit using correction terms with fixed exponents -3 and -4; the resulting estimates of μ_c are then subjected to a three-point fit with variable exponent such as in Eq. (19). This process can be iterated several times; Fig. 2 shows the exponents of subsequent corrections obtained in this way.

While the results obtained above for the exponents x_j are not very accurate, it is possible to apply more sensitive tests. For instance we may assume $x_2=-4$ and $x_3=-5$ in the first step, to obtain iterated estimates of x_1 by a three-point fit to the resulting values of μ in the next step. These estimates rapidly approach the value -3 to within 10^{-2}; another iteration by means of a three-point fit with a variable exponent decreases this numerical margin by another order of magnitude.

Similarly one can assume $x_1=-3$ and $x_3=-5$ and then focus on the determination of x_2; the resulting estimates are found to approach the value -4 to within 3×10^{-3}.

The results suggest that the spectrum of finite-size correction exponents is $x_j=-2-j$. This reveals a difference with respect to the spectrum of the exactly solved Ising model, where only corrections with odd j occur; this follows from a finite-size expansion [17] of the transfer-matrix eigenvalues as given e.g., by Domb [18]. A fit procedure involving such correction exponents for $j=1$ to 8 yields $\mu_c=1.334\,015\,100\,278\ (1)$.

Next, we consider the solutions for X_h, denoted as $X_h^{(0)}(L)$, of the equation $X_h(\mu,L+1)-X_h(\mu,L-1)=0$. These first estimates (see Table I) are already found to approach the value $X_h=1/8$ to within four decimal places. This is in a good agreement with the universal finite-size amplitude of the magnetic correlation length of the exactly solved Ising model, and also with earlier numerical results for the hard-square lattice gas.

The finite-size dependence of the $X_h^{(0)}(L)$ is closely related to that of $\mu^{(0)}(L)$, as follows from the substitution of Eq. (20) in Eq. (16):

$$X_h(\mu^{(0)},L)=X_h+a_1L^{z_1}+a_2L^{z_2}+a_3L^{z_3}+\cdots. \tag{21}$$

The exponents z_j in Eq. (21) are equal to $-j-1$ if $y_t=1$ and $y_i=-2$, as in the Ising model, and if $x_j=-2-j$ as above. Indeed, power-law extrapolation analogous to Eq. (19) shows that $z_1\approx-2$; furthermore it confirms that $X_h=1/8$ in six decimal places.

In analogy with the analysis of μ_c we have assumed $z_1=-2$, found that z_2 is close to -3, assumed that $z_2=-3$, and so on. We proceed to determine the X_h on the basis of Eq. (21) and the assumption $z_j=-j-1$. Thus we solve for the three unknowns $X_h^{(1)}(L)$, $a_1^{(1)}(L)$, and $a_2^{(1)}(L)$ in the three equations

$$X_h^{(0)}(L+l)=X_h^{(1)}(L)+a_1^{(1)}(L)(L+l)^{z_1^{(1)}}+a_2^{(1)}(L)(L+l)^{z_2^{(1)}}, \tag{22}$$

for $l=0$ and ±2, with $z_1^{(1)}=-2$ and $z_2^{(1)}=-3$. This leads to a sequence of iterated estimates $X_h^{(1)}(L)$ which is shorter than the original sequence (two less entries) but converges faster. On the basis of Eq. (21) with $z_j=-1-j$ we expect that, in leading orders, the $X_h^{(1)}(L)$ behave similarly as Eq. (22), but with different exponents

$$X_h^{(1)}(L+l)=X_h^{(2)}(L)+a_1^{(2)}(L)(L+l)^{z_1^{(2)}}+a_2^{(2)}(L)(L+l)^{z_2^{(2)}}, \tag{23}$$

with $z_1^{(2)}=z_3=-4$ and $z_2^{(2)}=z_4=-5$. From Eq. (23) we can now similarly solve for $X_h^{(2)}(L)$ on the basis of three values $X_h^{(1)}(L+l)$ for $l=0$ and ±2. This procedure can be carried on until $z_1^{(4)}=-8$, $z_2^{(4)}=-9$. Then we have applied a three-point fit with a variable exponent $z^{(5)}(L)$ by solving

$$X_h^{(4)}(L+l)=X_h^{(5)}(L)+a_1^{(5)}(L)(L+l)^{z^{(5)}(L)}. \tag{24}$$

This fit seems to converge rapidly with increasing L; we estimate $X_h=0.125\,000\,000\,000\ (1)$.

B. Determination of the critical point

Next we attempt to find the critical point more precisely by analyzing the finite-size data $X_h(\mu,L)$ for the magnetic

scaled gap, under the assumption that $X_h = 1/8$ holds exactly. We have thus solved the scaling equation $X_h(\mu, L) = 1/8$ numerically. This procedure offers the advantage that it is more stable with regard to the limited numerical precision of the calculation. The solutions for μ are denoted $\mu^{(0)}(L)$ (note that this notation has a different meaning than in the preceding subsection) and listed in Table II of Ref. [16]. Just as in the preceding subsection we find that the solutions behave in accordance with Eq. (20) with $x_j = -2-j$ (but with different amplitudes b_j). We thus proceed to determine the critical point on this basis. Combining two of these corrections at a time, we solve for the three unknowns $\mu^{(1)}(L)$, $b_1^{(1)}(L)$, and $b_2^{(1)}(L)$ in the three equations

$$\mu^{(0)}(L+l) = \mu^{(1)}(L) + b_1^{(1)}(L)(L+l)^{x_1^{(1)}} + b_2^{(1)}(L)(L+l)^{x_2^{(1)}}, \tag{25}$$

for $l = 0$ and ± 2, where $x_1^{(1)} = -3$ and $x_2^{(1)} = -4$. This in effect eliminates the corrections with powers -3 and -4 and thus $\mu^{(1)}(L)$ converges much faster with L than $\mu^{(0)}(L)$. On the basis of Eq. (20) with $x_j = -2-j$ we expect that the $\mu^{(1)}(L)$ behave similarly as Eq. (25), but with different exponents

$$\mu^{(1)}(L+l) = \mu^{(2)}(L) + b_1^{(2)}(L)(L+l)^{x_1^{(2)}} + b_2^{(2)}(L)(L+l)^{x_2^{(2)}}, \tag{26}$$

with $x_1^{(2)} = x_3 = -5$ and $x_2^{(2)} = x_4 = -6$. From Eq. (26) we can now similarly solve for $\mu^{(2)}(L)$ on the basis of three values $\mu^{(1)}(L+l)$ for $l = 0$ and ± 2. This procedure can be carried on until $x_1^{(4)} = -9$, $x_2^{(4)} = -10$. Then we have applied a three-point fit with a variable exponent $x^{(5)}(L)$ by solving

$$\mu^{(4)}(L+l) = \mu^{(5)}(L) + b_1^{(5)}(L)(L+l)^{x^{(5)}(L)}, \tag{27}$$

for $l = 0$ and ± 2. This yields our best estimate for the critical point as $\mu_c = 1.334\,015\,100\,277\,74\,(1)$, which is consistent with earlier analyses [9,10] and the result in the preceding subsection.

An indication for the correctness of our choice of the correction exponents follows from the behavior of $x^{(5)}$ as a function of L. Its values did not exceed $x_2^{(4)} = -10$. If we had used a wrong choice missing a significant correction $b_m L^{x_m}$, then we would have found $x^{(5)} \approx x_m$, as may be checked analytically and empirically. For instance, we have repeated the fitting procedure for μ_c using a different spectrum $x_j = -1-2j$. The missing exponent -4 then immediately turns up in a three-point fit with a variable exponent. These three-point fits provide a means to check the validity of the assumed spectrum and were applied at several stages of the iterated fitting procedure. These tests also provide a sensitive test to reveal, in addition to missing exponents, possible logarithmic factors in the dominant corrections. No signs of such factors were seen.

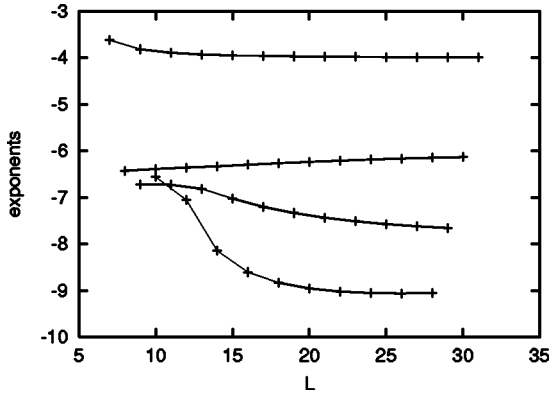

FIG. 3. Exponents of finite-size corrections in the critical free energy, versus finite size L. These exponents were obtained by means of three-point fits with a variable exponent, in different iteration steps. From above: (1) fit of the free energy; (2) after one iteration step using a fixed exponent -4; (3) after two iteration steps with exponents -4 and -6, and so on.

C. Bulk free energy and critical density

To determine the critical parameters of the present hard-square model, we have calculated the free energy per site and the density of particles at the extrapolated critical point for system sizes up to $L = 34$. These numerical results are shown in Table III of Ref. [16]. The critical free-energy density $f(L)$ is expected to depend on the finite size L as

$$f(L) = f_\infty + \frac{\pi c}{6L^2} + p_1 L^{y_1} + p_2 L^{y_2} + \cdots, \tag{28}$$

where the universal finite-size amplitude c may be identified with the conformal anomaly [19] in the case of conformally invariant models. The exponents $y_j < 0$ of the correction terms are, in principle, unknown. As in the preceding subsection we have attempted to determine dominant correction exponents. We find that $y_1 = -4$ with a numerical uncertainty of 0.01. After an iterated two-point fit with fixed exponent $y_1 = -4$, another iteration step by means of a three-point fit yields the next exponent as $y_2 = -6$ with a numerical uncertainty of 0.1. However, the next exponent y_3 could not be accurately determined. See Fig. 3. We included a correction with exponent $y_3 = -8$; if we fail to do so, three-point fits in a later iteration step reveal that an exponent is missing.

These findings would suggest the same spectrum as occurs in the free energy of the Ising model [17], namely, $y_j = -2-2j$. However, after a next iteration step for the lattice-gas free energies, with exponents -10 and -12, a three-point fit indicated the presence of a correction with an exponent close to -7.8, with a small amplitude. This hints at the presence of a small contribution proportional to $L^{-8}\ln L$, or perhaps at the presence of odd powers of L. The small magnitude of this effect does not allow us to make a more firm statement.

Thus, in analogy with the procedure to determine the critical point, more rapidly converging estimates of the bulk free

TABLE II. Best estimates of the conformal anomaly c, the magnetic scaling dimension X_h, the temperature scaling dimension X_t, the critical chemical potential μ_c, the critical bulk free energy $f(\mu_c)$, and the critical particle density $\rho(\mu_c)$ of the hard-core lattice-gas model.

c	X_h	X_t
0.500 000 000 000 0 (1)	0.125 000 000 000 0 (1)	1.000 000 000 00 (1)
μ_c	$f(\mu_c)$	$\rho(\mu_c)$
1.334 015 100 277 74 (1)	0.791 602 643 166 112 (1)	0.367 742 999 041 0 (3)

energy are obtained by solving the unknowns $f^{(1)}(L)$, $p_1^{(1)}$, and $p_2^{(1)}$ in

$$f^{(0)}(L+l)=f^{(1)}(L)+p_1^{(1)}(L)(L+l)^{y_1^{(1)}}+p_2^{(1)}(L)(L+l)^{y_2^{(1)}}, \tag{29}$$

where $f^{(0)}(L)\equiv f(L)$, $y_1^{(1)}=-2$, and $y_2^{(1)}=-4$, in the three equations for $l=0$ and ± 2. Iterated fits, using exponent pairs $(-6,-8)$, . . . , $(-14,-16)$, followed by a three-point fit with a free exponent as in Eq. (27), lead to our best estimate for the bulk free energy f_∞. It is included in Table II.

The particle density ρ plays the role of the energy in the Ising model. However, our numerical data for the critical density ρ_c display a clear finite-size dependence, while the energy of the exactly solved critical Ising model on a cylinder is independent of the finite size. Three-point fits to the densities computed at the critical point yield clear evidence for an exponent -4. However, after a fit with a fixed exponent -4 in the first step, a three-point fit to the resulting values of ρ yields *another* exponent close to -4 (with increasing system sizes it approaches this value within 0.1). The use of an exponent a little different from -4, e.g., -4.1, in the first step, makes only little difference. One still finds estimates of a next exponent that approach -4 within 0.1. These findings indicate that the term with power -4 is actually a combination of two terms with powers that are (almost) coincident. The simplest interpretation is the presence of a logarithmic term $L^{-4}\ln L$, although we cannot exclude the presence of a small fractional power in the system size L. The next exponent of L is found to be close to -6, but again modified with a similar factor resembling a logarithm. We thus performed the finite-size analysis of ρ_c on the basis of the formula

$$\rho(L)=\rho_c+u_1L^{-4}\ln(v_1L)+u_2L^{-6}\ln(v_2L)+\cdots. \tag{30}$$

As implied above, fits without such logarithmic factors fail to converge satisfactorily. The first iteration step in the determination of ρ_c is to solve for $\rho^{(1)}(L)$, $u_1^{(1)}(L)$, and $v_1^{(1)}(L)$ in

$$\rho^{(0)}(L+l)=\rho^{(1)}(L)+u_1^{(1)}(L)(L+l)^{x^{(1)}}\ln[v_1^{(1)}(L)(L+l)], \tag{31}$$

for $l=0$ and ± 2, using $x^{(1)}=-4$, on the basis of the finite-size data $\rho^{(0)}(L)$ for ρ_c as calculated at the estimated critical point. The next iteration steps proceed similarly, but with exponents $x^{(2)}=-6$, and $x^{(3)}=-8$. This leads to the extrapolated critical density shown in Table II.

D. Conformal anomaly and critical exponents

On the basis of Eq. (28) we obtain estimates of the free-energy amplitude c by solving the unknowns $f^{(1)}(L)$ and $c^{(0)}(L)$ in

$$f^{(0)}(L+l)=f^{(1)}(L)+\frac{\pi c^{(0)}(L)}{6(L+l)^2}, \tag{32}$$

for $l=\pm 1$ and a range of odd values of L, using the available finite-size results for $f^{(0)}(L+l)=f(L+l)$ at the estimated critical point. The next iteration step is to solve the equations

$$c^{(0)}(L+l)=c^{(1)}(L)+d_1^{(1)}(L)(L+l)^{x_1^{(1)}}+d_2^{(1)}(L)(L+l)^{x_2^{(1)}}, \tag{33}$$

for $l=0$ and ± 2, with $x_1^{(1)}=-2$ and $x_2^{(1)}=-4$, in accordance with Eq. (28) and the aforementioned values of y_j therein. Following iteration steps used exponent pairs $(-6,-8)$, . . . , until $(-14,-16)$. However, three-point fits then reveal a "missed" correction with exponent -6 which corresponds with a term proportional to $L^{-8}\ln L$ as mentioned in the analysis of the free energy. After including this correction, the resulting best estimate for the free-energy amplitude c is included in Table II.

Our transfer-matrix calculations include results for the magnetic and energy-energy correlation lengths, $\xi_h(L)$ and $\xi_t(L)$, respectively, at the calculated critical point. These results are shown in Table IV of Ref. [16] in terms of the scaled magnetic gaps $X_h^{(0)}(L)\equiv L/[2\pi\xi_h(L)]$ and the scaled thermal gaps $X_t^{(0)}(L)\equiv L/[2\pi\xi_t(L)]$. Finite-size-scaling predicts the following finite-size dependence of the scaled magnetic gap:

$$X_h^{(0)}(L)=X_h+b_1L^{y_1}+b_2L^{y_2}+\cdots, \tag{34}$$

and a similar relation for the scaled thermal gap. The finite-size amplitudes X_h and X_t are universal numbers. For models with conformally invariant fixed points, they are equal to the magnetic scaling dimension [20] $2-y_h$ and the temperature scaling dimension $2-y_t$, respectively.

In accordance with our findings in Sec. III A, we assume that the spectrum $z_j=-1-j$ applies. The first iteration step thus involves the solution of

$$X_h^{(0)}(L+l)=X_h^{(1)}(L)+b_1^{(1)}(L)(L+l)^{z_1^{(1)}}+b_2^{(1)}(L)(L+l)^{z_2^{(1)}}, \tag{35}$$

for $l=0$ and ± 2, with $z_1^{(1)}=-2$ and $z_2^{(1)}=-3$. The iteration process can be continued until $z_1^{(6)}=-12$ and $z_2^{(6)}=-13$, followed by a three-point fit with a free exponent as in Eq. (27). The final result is shown in Table II.

For the scaled thermal gaps, we have applied the same iterated fit procedure with the same series of correction exponents. The extrapolated finite-size amplitude is included in Table II.

E. Test of conformal invariance

The interpretation of the universal correlation length amplitudes X_h and X_t in terms of the scaling dimensions is only valid in conformally invariant models. In the absence of a proof of conformal invariance, one can still determine the scaling dimensions independently by means of numerical differentiation of the free energy and the scaled gap. From the μ dependence of the magnetic gap, Kamieniarz and Blöte [9] obtained the temperature renormalization exponent as $y_t=1.000\,01\ (2)$ while Todo and Suzuki [10] reported $y_t=0.999\,9\ (3)$. This is in a good agreement with the interpretation of X_t as the temperature scaling dimension $2-y_t$. Here we extend this test to include second derivatives of the free energy and the scaled gap with respect to μ and the staggered chemical potential $\mu_{\rm st}$, which plays the role of the magnetic field in the Ising model.

Including magnetic and temperature scaling fields h and t, respectively, Eq. (28) becomes

$$f(h,t,L)=f_a(h,t)+L^{-2}\tilde{f}(L^{y_h}h,L^{y_t}t)+\sum_j t_j L^{y_j}+\cdots, \tag{36}$$

where f_a is the analytic part of the free-energy density, and $\tilde{f}$ is the finite-size-scaling function of the singular part of the free-energy density. Expansion of $\tilde{f}$, which is supposed to be analytic, in powers of h and t yields the dominant finite-size-scaling behavior of the derivatives of $f(h,t,L)$. Corrections arise due to t dependence of the coefficients t_j on h and t. Similarly we include the dependence of the scaled magnetic gap on h and t,

$$X_h(h,t,L)=\tilde{X}(L^{y_h}h,L^{y_t}t)+\sum_j a_j L^{y_j}+\cdots, \tag{37}$$

where also the scaling function $\tilde{X}$ is supposed to be analytic. Up to irrelevant corrections, we may associate t with the distance $\mu-\mu_c$ to the critical point, and h with the staggered chemical potential $\mu_{\rm st}$. The finite-size correction amplitudes a_j are still dependent on h and t.

Thus we obtained free energies and scaled gaps at $\mu_{\rm st}=0$ for a range of values of μ about the critical point μ_c, and also for a range of values of $\mu_{\rm st}$ about 0 at $\mu=\mu_c$. Polynomials in $\mu-\mu_c$ and $\mu_{\rm st}$ (up to eighth order) were fitted to these results. The widths of the ranges were chosen such as to optimize the numerical precision of the results for the derivatives of f and X. These calculations were performed in double-precision arithmetic, for even system sizes up to $L=30$. The numerical differentiations have to be restricted to relatively narrow ranges (about 10^{-2} to 10^{-3}), which leads to a loss of accuracy of several decimal places. The numerical analyses, which are only briefly summarized below, involve iterated fitting procedures. Each iteration step increases the numerical inaccuracy even further, so that only a few steps are feasible.

(1) According to Eq. (36), at $\mu=\mu_c$, $\mu_{\rm st}=0$ the specific-heat-like quantity $\partial^2 f/\partial\mu^2$ behaves as

$$\frac{\partial^2 f}{\partial\mu^2}=c_0+L^{2y_t-2}(r_0+r_1L^{y_i}+\cdots). \tag{38}$$

Three-point fits, with c_0, r_0, and the exponent y_t as free parameters and ignoring further contributions, show that the result for y_t rapidly approaches 1 with increasing L; the difference is only 6×10^{-4} for the largest value of L. Results of iterated three-point fits converge even faster, and the estimated values of y_t now approach 1 up to 5×10^{-6}. Moreover, the iterated fits reveal that the correction exponent y_i is close to -2.

(2) At the critical point $\mu=\mu_c$, $\mu_{\rm st}=0$ we expect that the susceptibilitylike quantity $\partial^2 f/\partial\mu_{\rm st}^2$ behaves similarly as Eq. (38), but with y_t replaced by y_h. Three-point fits lead to estimates of y_h rapidly approaching 15/8 with increasing finite sizes. The difference is about 10^{-4} for the largest available sizes. For iterated three-point fits, this difference decreases to 10^{-5}. Again, the results for y_i approach -2.

(3) Analysis of the derivatives of the scaled gap (or the correlation length) has the advantage that an "analytic" background is absent. The first derivative to the chemical potential should, according to Eq. (37), satisfy

$$\frac{\partial X}{\partial\mu}=L^{y_t}(t_0+t_1L^{y_i}+\cdots). \tag{39}$$

Two-point fits with y_t and t_0 as free parameters, and neglecting all other terms, yielded estimates of y_t rapidly approaching 1, with a difference of 4×10^{-4} for the largest pair of system sizes. After an iteration step using three-point fits, the difference decreases to 10^{-5}, while the results for y_i again approach -2.

(4) Similarly, we expect for the second derivative of the scaled gap that

$$\frac{\partial^2 X}{\partial\mu^2}=L^{2y_t}(q_0+q_1L^{y_i}+\cdots). \tag{40}$$

Two-point fits with y_t and q_0 as free parameters produce estimates of y_t that approach 1, but more slowly than for the first derivative: the difference is still 10^{-2} for the largest system sizes. A second iteration step using three-point fits reduces the difference to 5×10^{-4}, and a third step to 2×10^{-5}.

(5) The scaled gap is an even function of $\mu_{\rm st}$, so that we focus on its second derivative. We expect similar behavior as

in Eq. (40) but with y_t replaced by y_h. Two-point fits show that the results for y_h rapidly approach 15/8, until a difference of 10^{-3} at the largest L values. After a second iteration involving three-point fits the difference reduces to about 10^{-5}, and after a third step to 10^{-6}.

The fits mentioned in this subsection lead to unbiased error estimates in the sense that they leave all the correction exponents free. We have made some additional fits with correction exponents fixed according to their value in the exactly solved Ising model (and consistent with the values found with iterated fits). In a few cases, an additional iteration step then becomes possible, which then produces values for y_t and y_h that approach the exact Ising values even closer, by approximately one order of magnitude.

In the fits presented here, the difference between subsequent estimates of y_t and y_h typically decreases rapidly with increasing system size L. Moreover, it tends to be roughly the same as the difference with the exact Ising values. Thus, we conclude that the numerical uncertainty in the largest-L results are of the same order as the differences with the Ising values as mentioned above.

IV. CONCLUSION

The numerical results in Table II are in a very precise agreement with the exactly known results $c=\frac{1}{2}$ for the finite-size amplitude of the free energy, and the scaled correlation lengths $X_h=\frac{1}{8}$ and $X_t=1$ of the Ising model. The numerical margin of uncertainty, as estimated from the differences between subsequent finite-size results in the last iteration step of the fitting procedure, is only 10^{-11} for X_t and 10^{-13} for c and X_h. We should mention another source of uncertainty, which is due to the procedures that we followed in various steps of this analysis. Namely, we have fixed some (in principle unknown) universal parameters in the fit formulas according to the exact solution of the Ising model. We believe that the resulting uncertainty is very limited for the following reasons. First, wherever we could determine these fixed parameters independently in the lattice-gas model, they agreed with our assumptions. Second, the fixed parameters are irrelevant in the sense that, even in the case of a wrong parameter choice, our fit procedures still must converge.

For instance, we have fixed the magnetic correlation length amplitude as $X_h=\frac{1}{8}$ in the determination of the critical point. This choice is supported by earlier analyses [1,9,10] and the independent determination of X_h in Sec. III A, but deviations of the order of 10^{-7} cannot be excluded on this basis. If (due to a hypothetical violation of universality) such a deviation exists for the present lattice gas, then the solutions of the equation $X_h(\mu,L)=1/8$ would obviously still converge to μ_c as long as $y_t>0$ in Eq. (21). In that case the speed of convergence would be affected, but no indications thereof were seen. Such a very small deviation could at most lead to an underestimation of the numerical uncertainty margins mentioned above. But it is reassuring that two different procedures to determine X_h, namely, those described in Secs. III A and III D, agree within the estimated margins of 10^{-12} or less.

The reliability and consistency of the fit procedures described in the preceding section was tested by introducing a number of variations in these procedures. For instance, instead of iteration steps involving two corrections, we may alternatively fit for one correction at a time. This yielded consistent results. For example, in the determination of c we have, besides Eq. (32), also used Eq. (29) in the first step. This led to a difference in the estimated value of c of less than 10^{-11}. Furthermore, the critical point was also analyzed using a sequence of exponents $x_j=-1-2j$ instead of those given under Eq. (21). While the result was consistent with that given above, the apparent convergence was less good and the answer therefore less convincing. In many cases we have applied three-point fits with a variable exponent in order to estimate the exponent of the next correction term. These checks provided strong support that our choices of the correction exponents, as well as that of $X_h=\frac{1}{8}$ in the determination of the critical point, were correct. It thus seems that the exponents of the finite-size corrections in the lattice-gas model include those of the solvable Ising model, but that there are also correction terms that are absent in the Ising model. Evidence for such corrections is found in the free energy and in the scaled gap. In particular, we find good evidence for terms modified by logarithmic correction factors in the critical density. It is interesting that logarithmic corrections in *thermodynamic* parameters have been proposed by Barma and Fisher [21], also in the context of Ising models outside the exactly solved category.

These new corrections need not be attributed to deviations from Ising universality. Their absence in the exactly solved Ising model can well be attributed to the vanishing of the corresponding amplitudes in the latter model. Indeed self-duality already implies that finite-size corrections are absent in the critical energies of these Ising systems on an infinitely long cylinder.

Thus we conclude that, from the viewpoint of universality, the set of correction exponents of the lattice gas is consistent with that of the exactly solved Ising model.

Assuming the validity of the spectrum of exponents as suggested by the numerical analysis of the correction terms, we obtain a few universal finite-size amplitudes that agree, within estimated numerical margins not exceeding 10^{-11}, with the exact Ising values. These results provide our most sensitive test of the Ising character of the lattice-gas model. Although the width of the estimated numerical error margin depends on the mentioned assumption, the fact remains that the numerical results agree in 11 decimal places with the exact Ising values. If the lattice gas were not in the Ising universality class, then it would seem extremely implausible that so many decimal places coincide. In this light we can be very confident that the lattice gas belongs to the Ising universality class.

If the renormalization fixed point of lattice-gas model is conformally invariant, one may interpret X_h and X_t as the magnetic and temperature scaling dimensions, respectively, and the scaled free-energy amplitude c as the conformal

anomaly. First, we note the fact that our analysis of the finite-size amplitudes agrees very precisely with the predictions for the $c=1/2$ conformal theory. In addition, we have performed independent tests, presented in Sec. III E, which confirm that the scaling dimensions indeed coincide with $X_t=1$ and $X_h=1/8$, and thereby provide further evidence that the theory of conformal invariance [22,23] applies to the present model.

Finally we remark that the classification of the present hard-square model in terms of Ising universality also supported by results for an amplitude ratio [24] defined on the distribution of the sublattice densities, in analogy with the Binder cumulant [25] for the Ising model.

ACKNOWLEDGMENTS

We thank the HPaC center in Delft for the use of computer facilities, in particular the Cray J-90 computer, and Jana Vasiljev for system support. This research was supported in part by the Dutch FOM (Fundamenteel Onderzoek der Materie) foundation, which is financially supported by the NWO (''Nederlandse Organisatie voor Wetenschappelijk Onderzoek''), and by the National Science Foundation of China under Grant No. 10105001. H.B. and W.G. gratefully acknowledge the hospitality of the Physics Department of the Beijing Normal University, and the Delft Computational Physics Section, respectively.

[1] H.W.J. Blöte and X.N. Wu, J. Phys. A **23**, L627 (1990).
[2] M.E. Fisher, J. Math. Phys. **4**, 278 (1963).
[3] R.J. Baxter, J. Phys. A **13**, L61 (1980).
[4] D.A. Huse, J. Phys. A **16**, 4357 (1983).
[5] D.S. Gaunt and M.E. Fisher, J. Chem. Phys. **43**, 2840 (1965).
[6] R.J. Baxter, I.G. Enting, and S.K. Tsang, J. Stat. Phys. **22**, 465 (1980).
[7] D.W. Wood and M. Goldfinch, J. Phys. A **13**, 2781 (1980).
[8] Z. Racz, Phys. Rev. B **21**, 4012 (1980).
[9] G. Kamieniarz and H.W.J. Blöte, J. Phys. A **26**, 6679 (1993).
[10] S. Todo and M. Suzuki, Int. J. Mod. Phys. C **7**, 811 (1996).
[11] A.C.D. van Enter, R. Fernández, and A.D. Sokal, J. Stat. Phys. **72**, 879 (1993).
[12] M.E. Fisher and M. Randeria, Phys. Rev. Lett. **56**, 2332 (1986).
[13] H.W.J. Blöte, J.R. Heringa, A. Hoogland, E.W. Meyer, and T.S. Smit, Phys. Rev. Lett. **76**, 2613 (1996).
[14] M.P. Nightingale, Phys. Lett. A **59**, 486 (1977); Proc. K. Ned. Akad. Wet., Ser. A: Math. Sci. **82**, 235 (1979).
[15] M.E. Fisher, Proceedings of International School of Physics ''Enrico Fermi,'' edited by M.S. Green (Academic, New York, 1971).
[16] See EPAPS Document No. E-PLEEE8-66-011211PRE for an appendix containing numerical data of extended numerical precision. A direct link to this document may be found in the online article's HTML reference section. The document may also be reached via the EPAPS homepage (http://www.aip.org/pubservs/epaps.html) or from ftp.aip.org in the directory /epaps/. See the EPAPS homepage for more information.
[17] N.Sh. Izmailian and Chin-Kun Hu, Phys. Rev. Lett. **86**, 5160 (2001).
[18] C. Domb, Adv. Phys. **9**, 149 (1960).
[19] H.W.J. Blöte, J.L. Cardy, and M.P. Nightingale, Phys. Rev. Lett. **56**, 742 (1986); I. Affleck, *ibid.* **56**, 746 (1986).
[20] J.L. Cardy, J. Phys. A **17**, L358 (1984).
[21] M. Barma and M.E. Fisher, Phys. Rev. B **31**, 5954 (1985).
[22] A.A. Belavin, A.M. Polyakov, and A.B. Zamolodchikov, J. Stat. Phys. **34**, 763 (1984).
[23] D. Friedan, Z. Qiu, and S. Shenker, Phys. Rev. Lett. **52**, 1575 (1984).
[24] G. Kamieniarz and H.W.J. Blöte, J. Phys. A **26**, 201 (1993).
[25] K. Binder, Z. Phys. B: Condens. Matter **43**, 119 (1981).